



The impact of nuclear shape on the emergence of the neutron dripline

Reference: Naofumi Tsunoda, Takaharu Otsuka, Kazuo Takayanagi, Noritaka Shimizu, Toshio Suzuki, Yutaka Utsuno, Sota Yoshida, Hideki Ueno, Nature 587, 66 (2020)

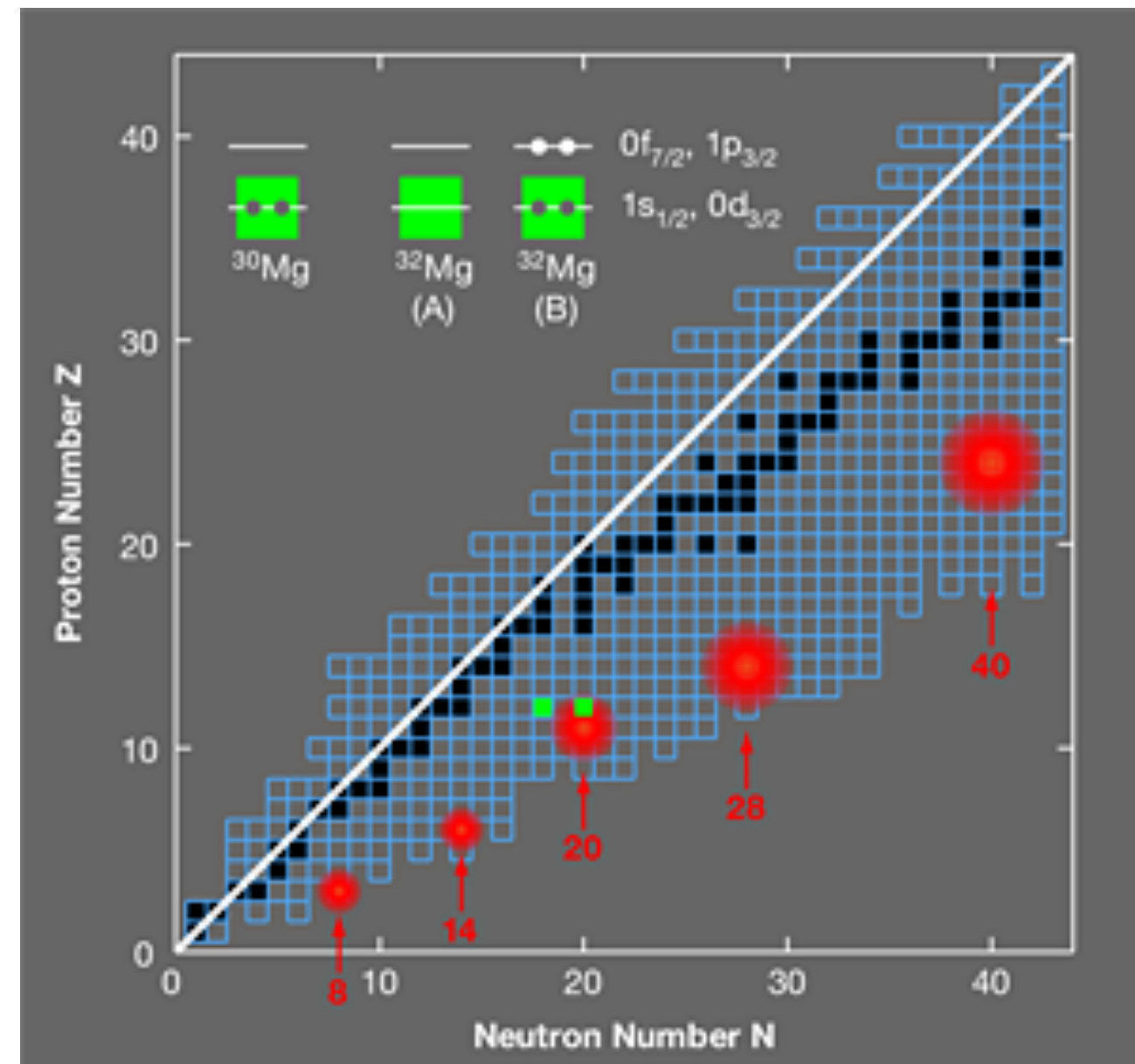
Jiangming Yao (尧江明)
中山大学物理与天文学院
School of Physics and Astronomy
Sun Yat-sen University

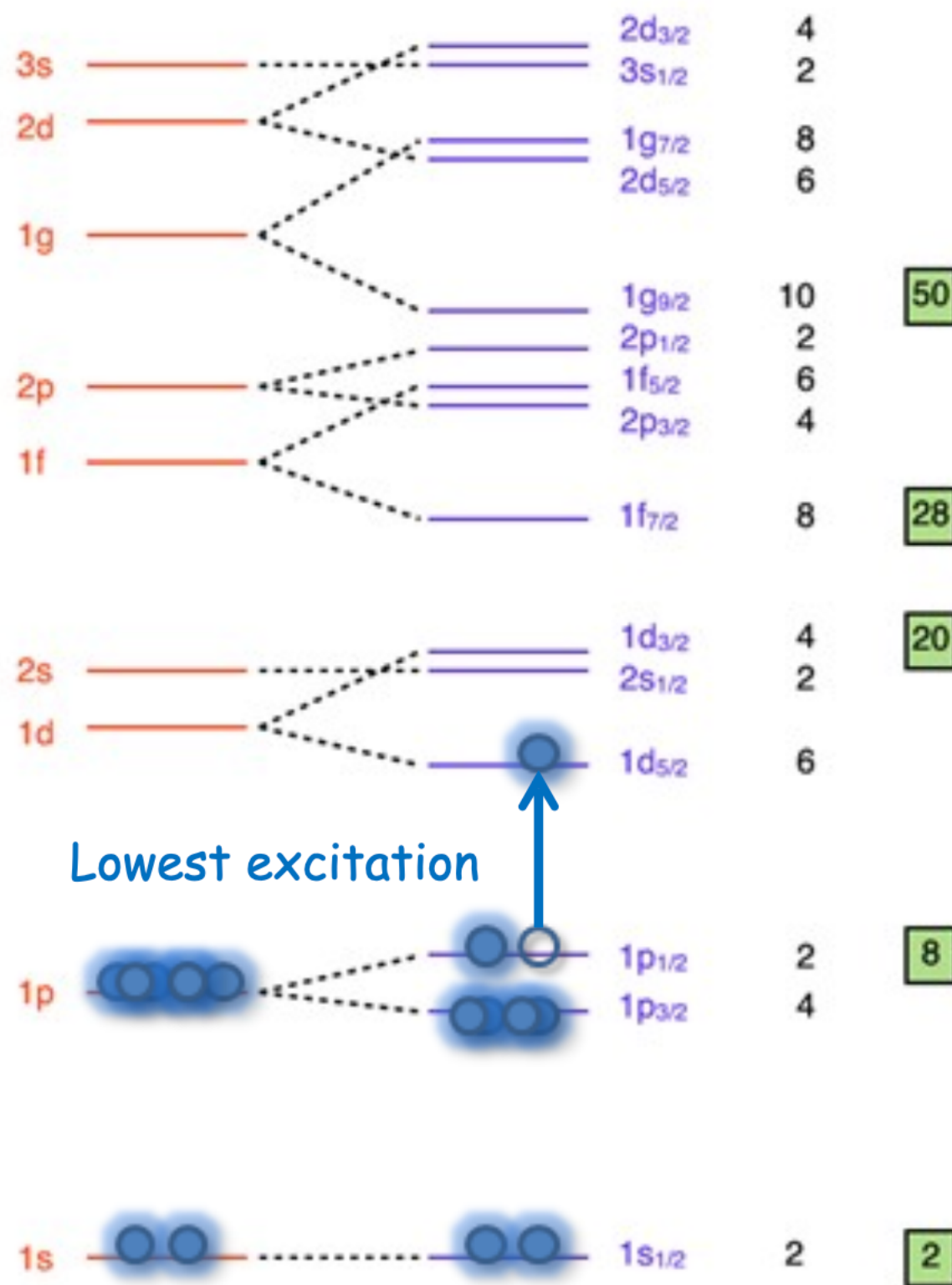


Island of inversion:

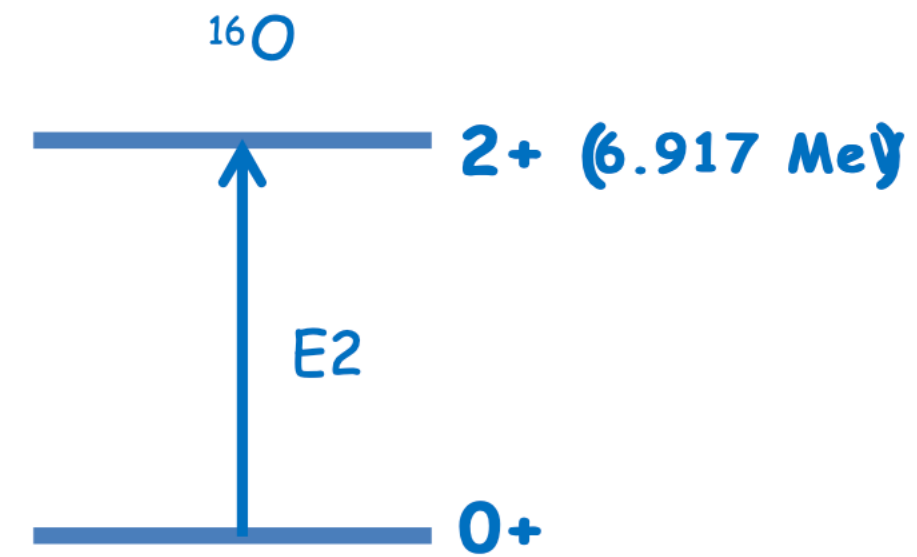
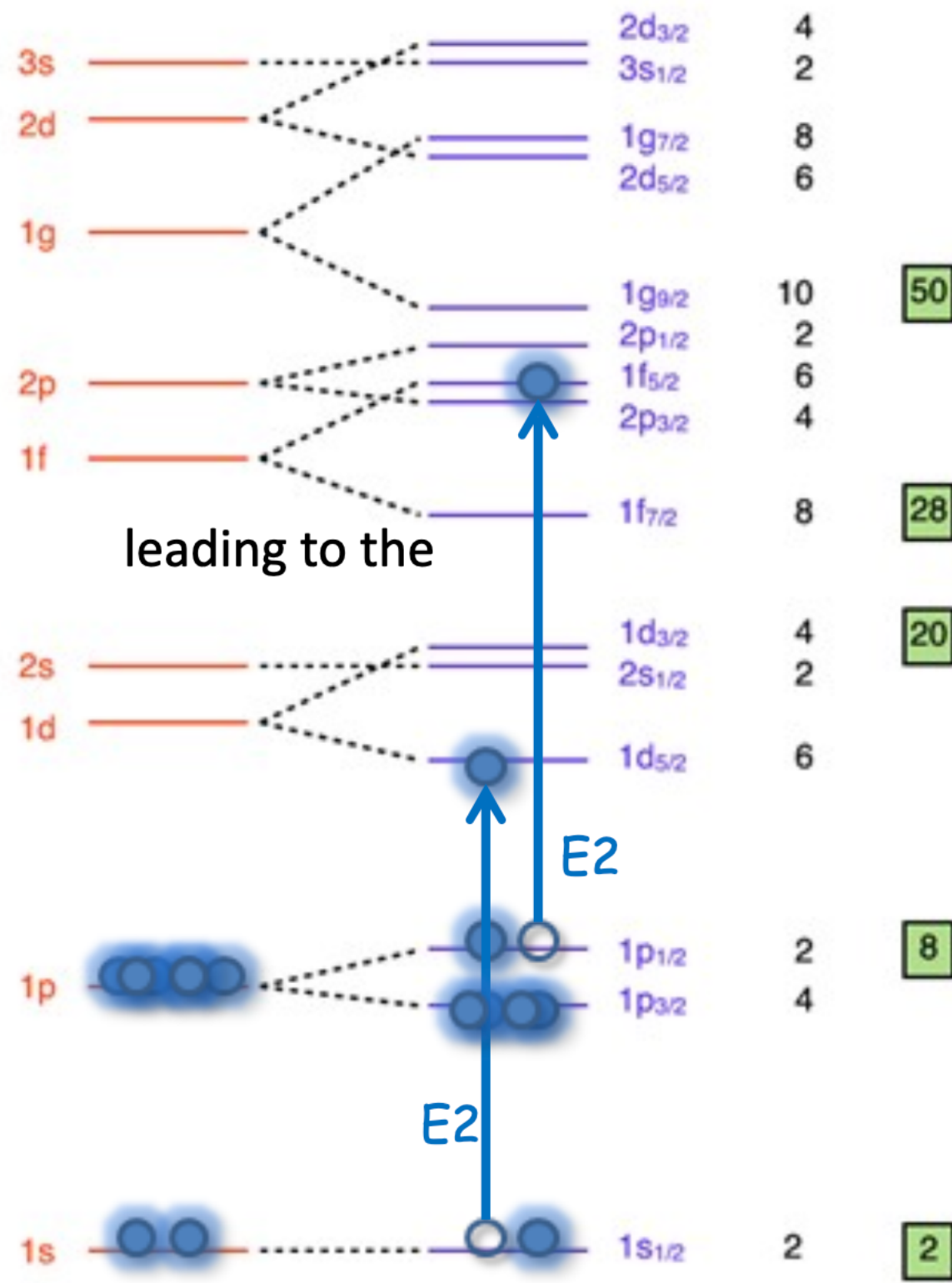
An island of inversion is a region of the chart of nuclides that contains isotopes with a **non-standard ordering of single particle levels in the nuclear shell model**. Such an area was first described in 1975 by French physicists carrying out spectroscopic mass measurements of exotic isotopes of lithium and sodium.

- Centered at neutron-rich isotopes of five elements 11Li, 20C, 31Na, 42Si, and 64Cr.
- Also called “**islands of shell breaking**” associated with the magic neutron numbers 8, 14, 20, 28, and 40.

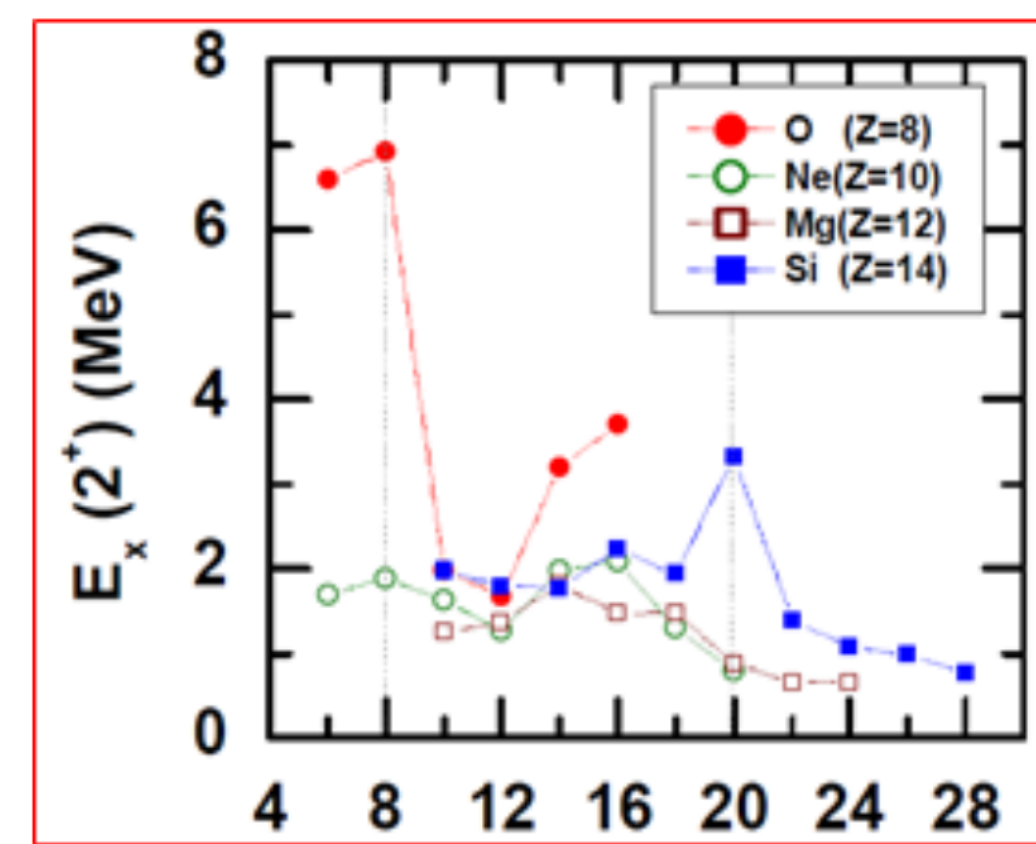




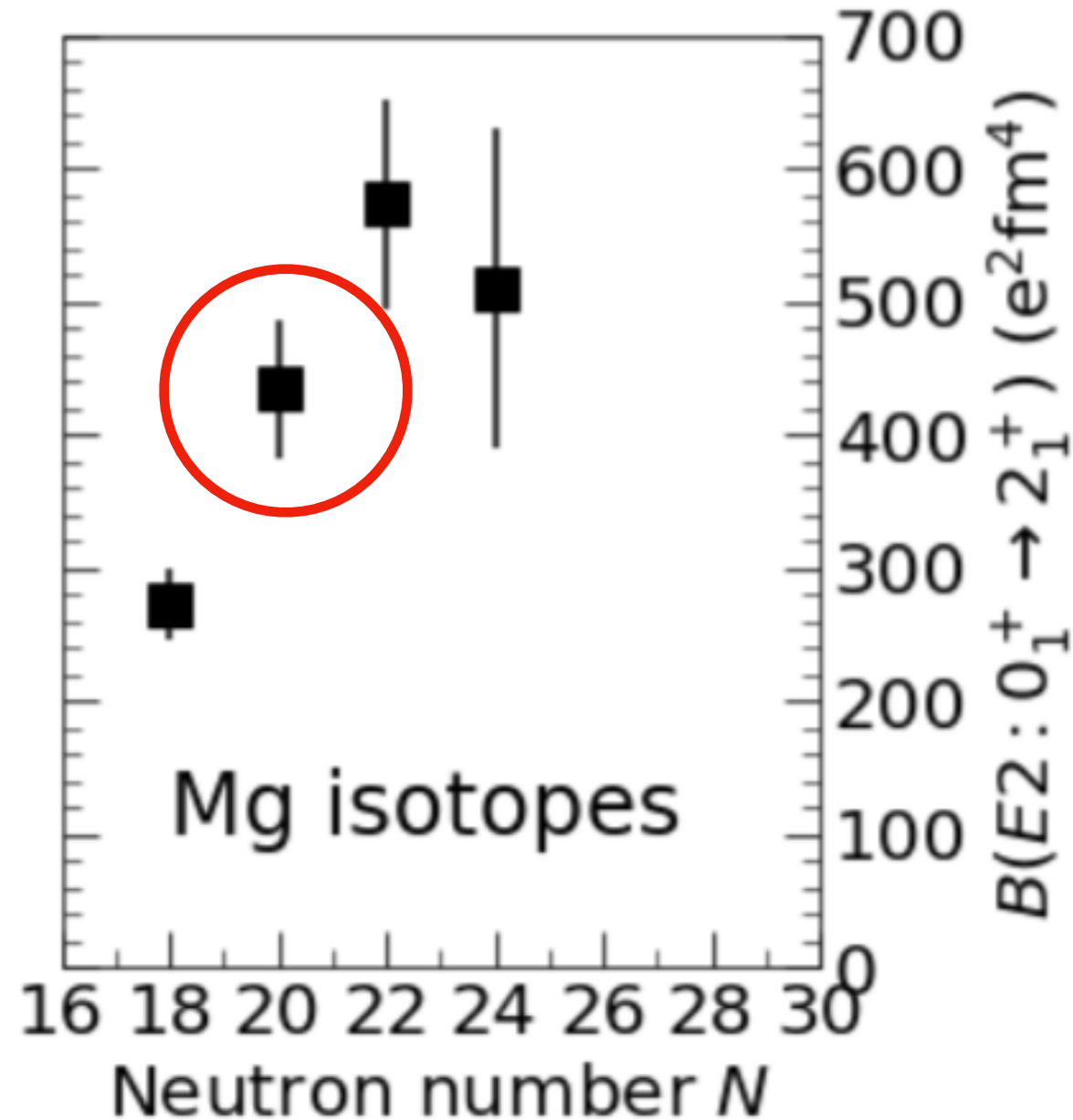
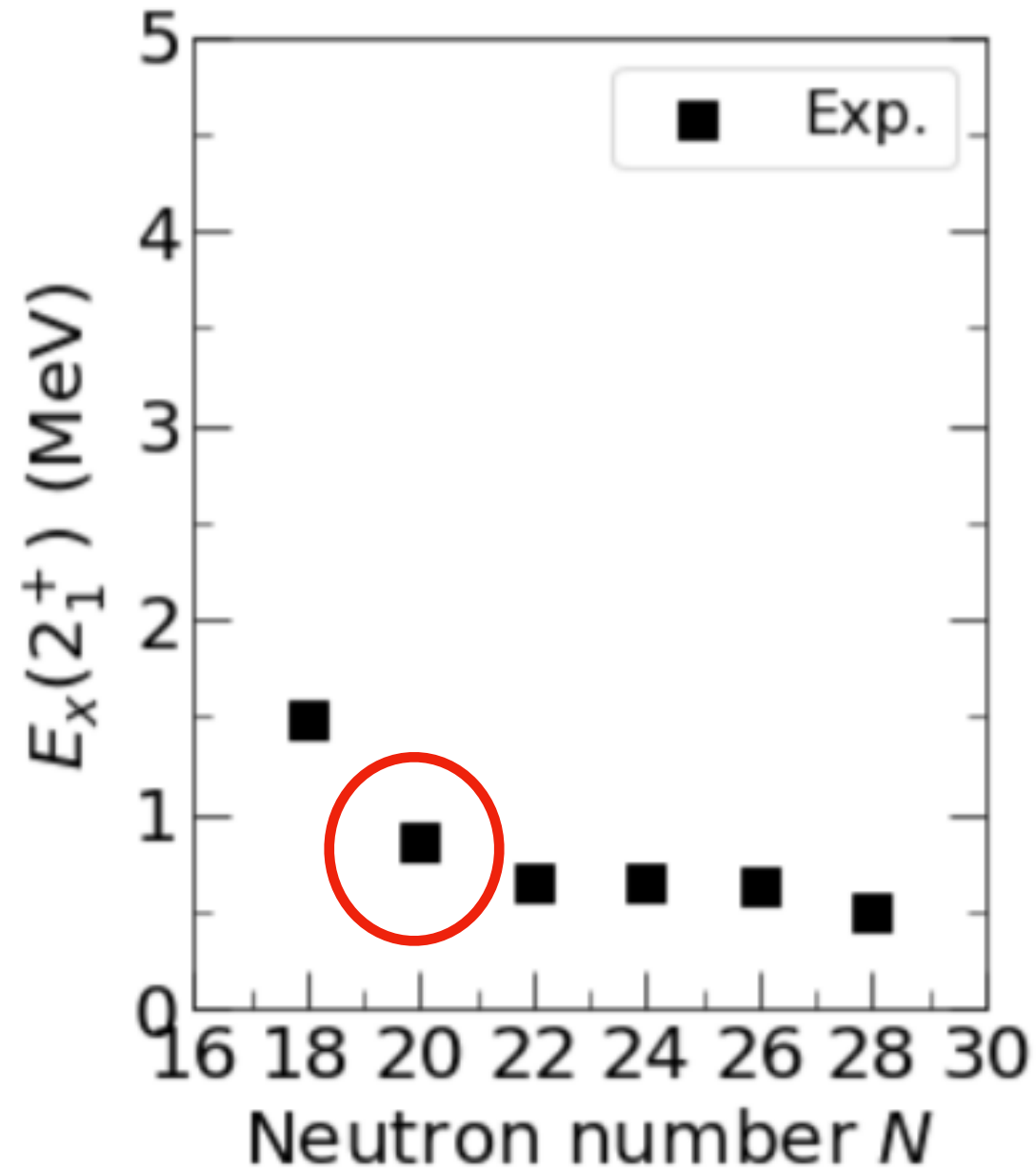
Introduction



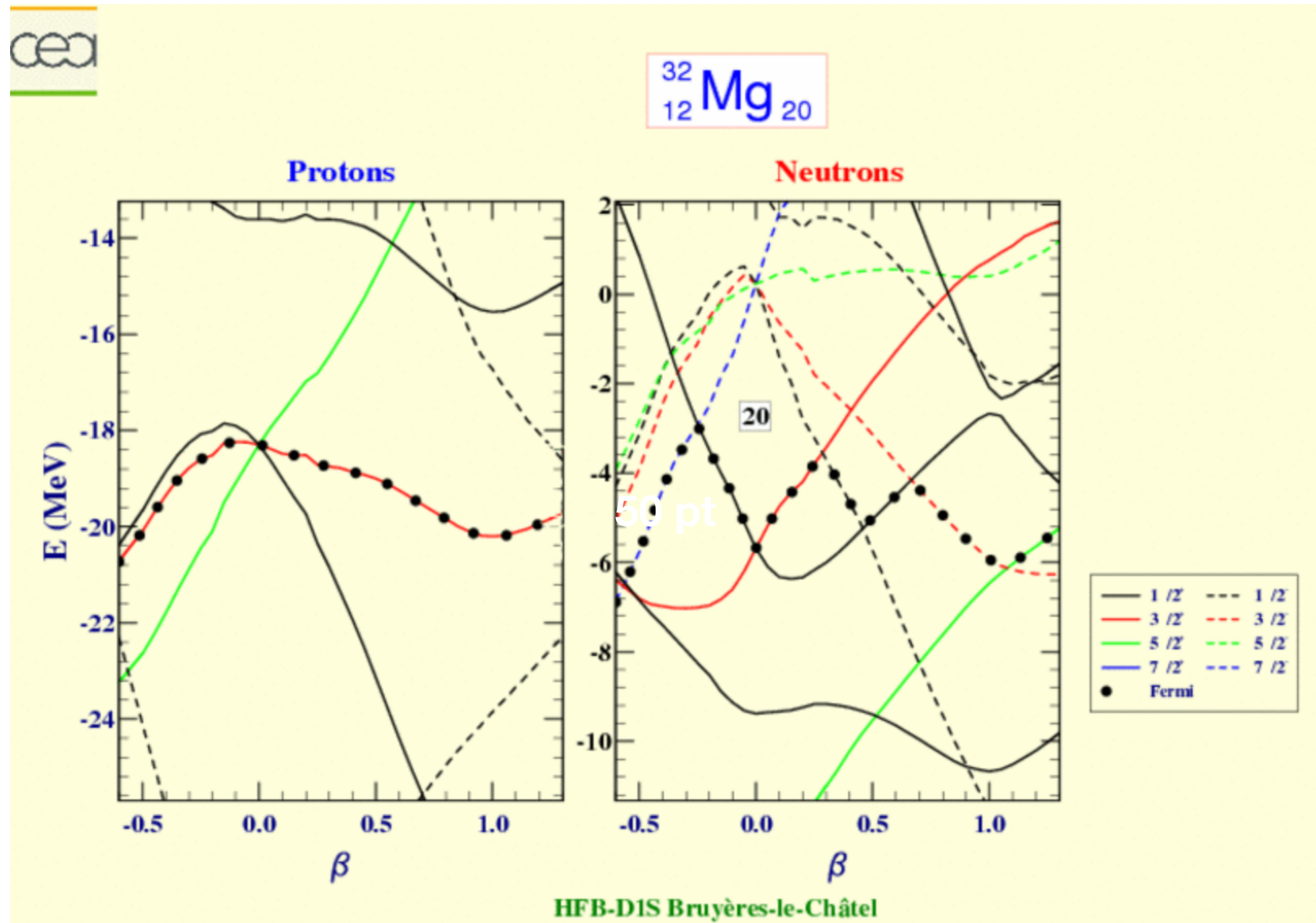
High excitation energy



Introduction

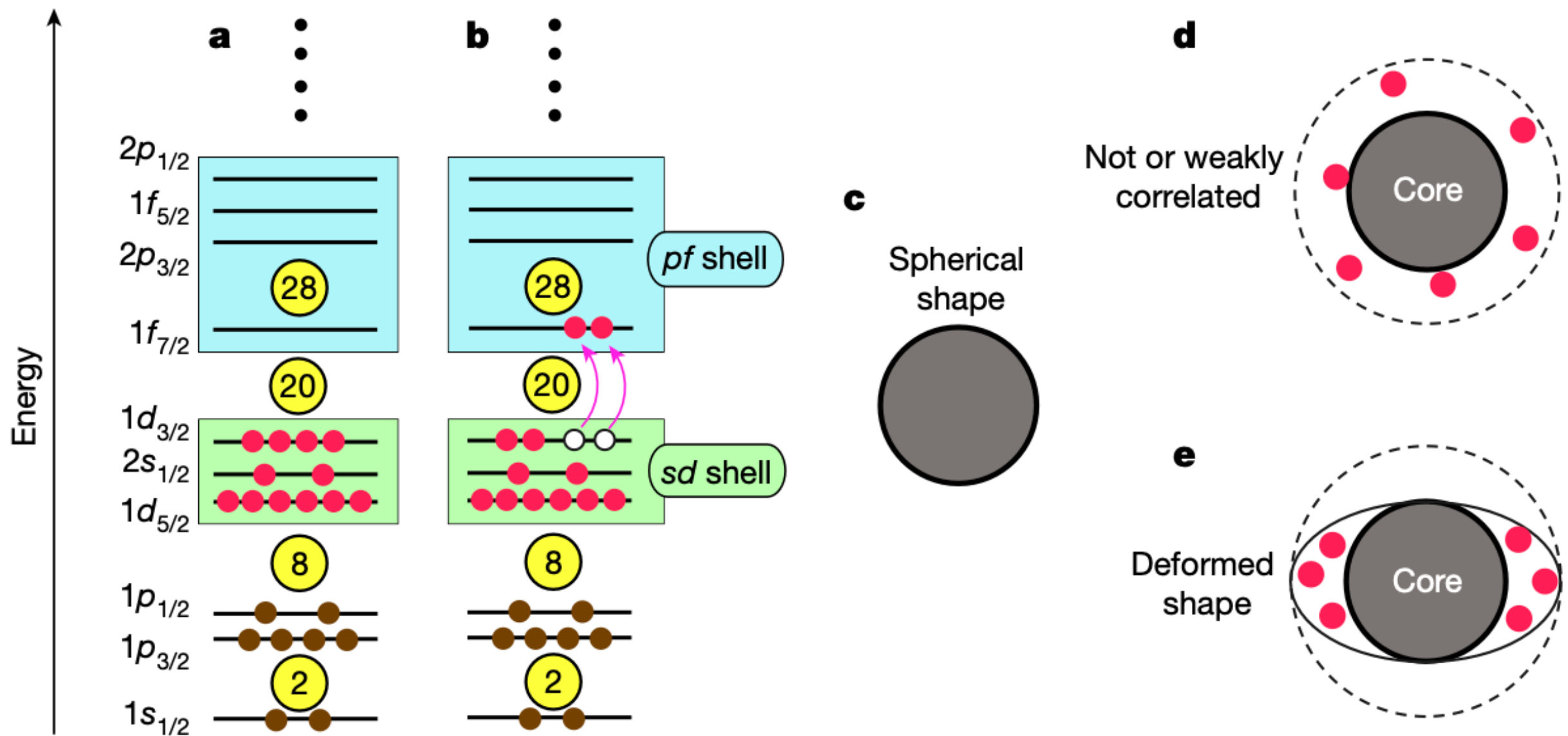


Introduction



The Nilsson diagram for protons or neutrons around $N = Z = 20$ with quadrupole deformation from the HFB calculation using the D1S force

Shell-model and nuclear shape



Cross-shell excitations: sd to pf shell

MCSM — Hubbard-Stratonovich (HS) Transformation

❖ “time” slices of β

$$e^{-\beta \hat{H}} = \left[e^{-\Delta \beta \hat{H}} \right]^{N_t}$$

❖ HS transformation

$$e^{-\beta \hat{H}} \simeq \prod_{n=1}^{N_t} \int_{-\infty}^{\infty} \prod_{\alpha} d\sigma_{\alpha n} \sqrt{\frac{\Delta \beta |V_{\alpha}|}{2\pi}} \cdot e^{-\frac{\Delta \beta}{2} |V_{\alpha}| \sigma_{\alpha n}^2} \cdot e^{-\Delta \beta (E_{\alpha} + s_{\alpha} V_{\alpha} \sigma_{\alpha n}) \hat{O}}$$

❖ Gaussian weight factor

$$G(\sigma_{\alpha}) = e^{-\frac{\Delta \beta}{2} |V_{\alpha}| \sigma_{\alpha n}^2}$$

❖ one-body Hamiltonian

$$\hat{h}(\sigma_n) = \sum_{\alpha} (E_{\alpha} + s_{\alpha} V_{\alpha} \sigma_{\alpha n}) \hat{O}_{\alpha}$$

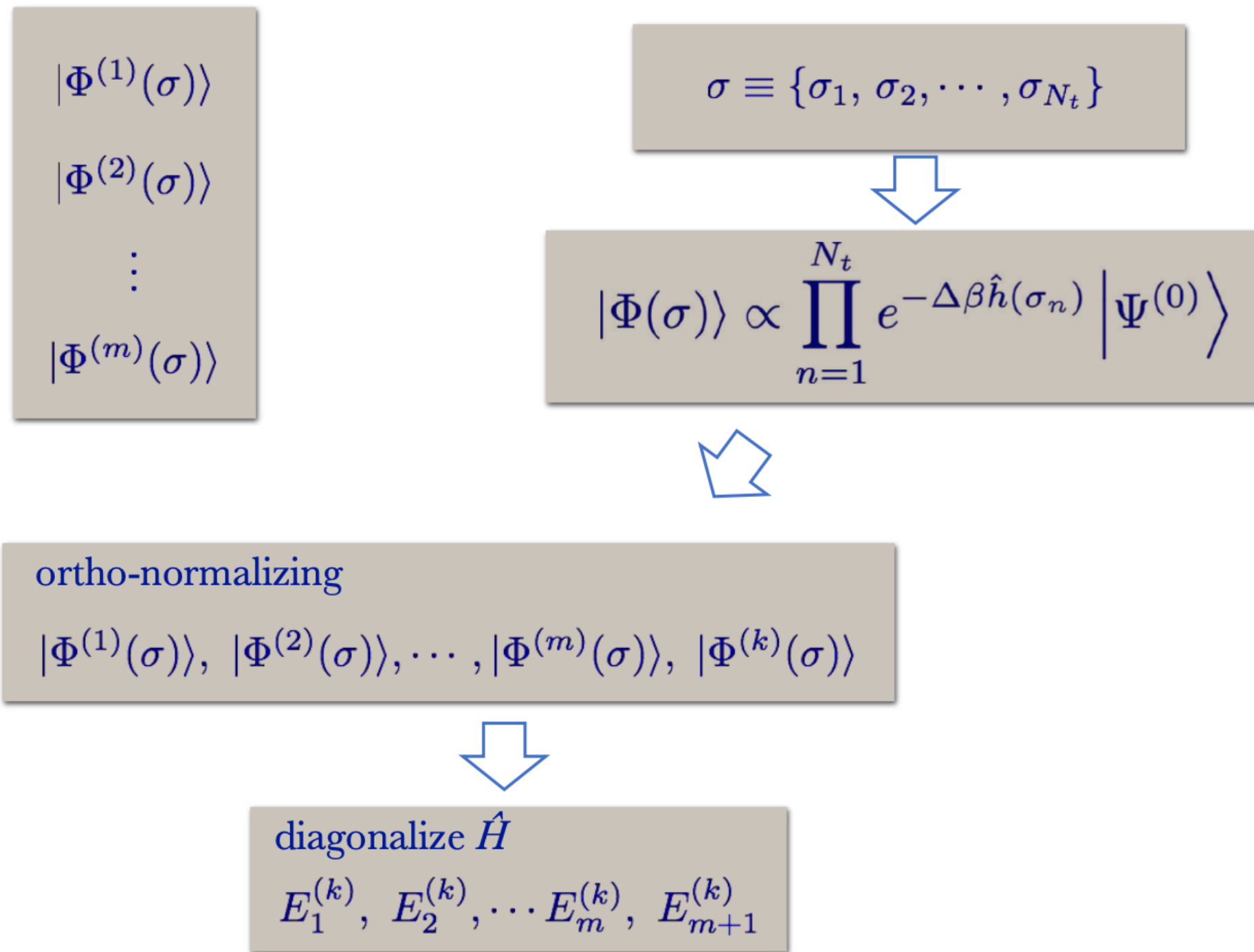
$s_{\alpha} = \pm 1$ ($\pm i$) if $V_{\alpha} < 0$ (> 0)

❖ HS transformation

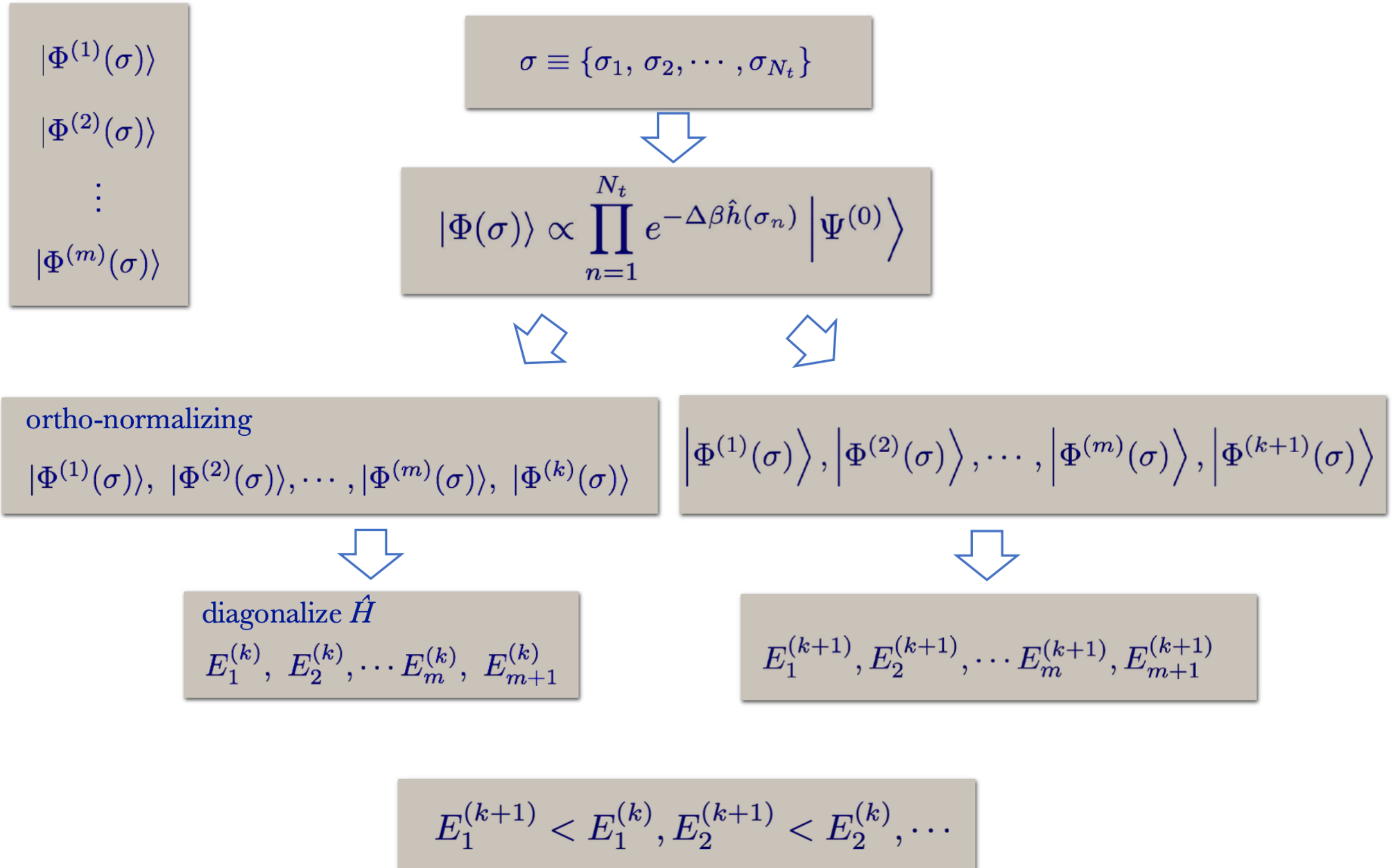
$$e^{-\beta \hat{H}} \simeq \prod_{n=1}^{N_t} \int_{-\infty}^{\infty} \prod_{\alpha} d\sigma_{\alpha n} \sqrt{\frac{\Delta \beta |V_{\alpha}|}{2\pi}} \cdot G(\sigma_{\alpha}) \cdot e^{-\Delta \beta \hat{h}(\sigma_{\alpha})}$$

R. L. Stratonovich, Dokl. Akad. Nauk SSSR **115**, 1097 (1957)
 [Sov. Phys. Dokl. **2**, 416 (1958)].

MCSM — Generation Process for Basis

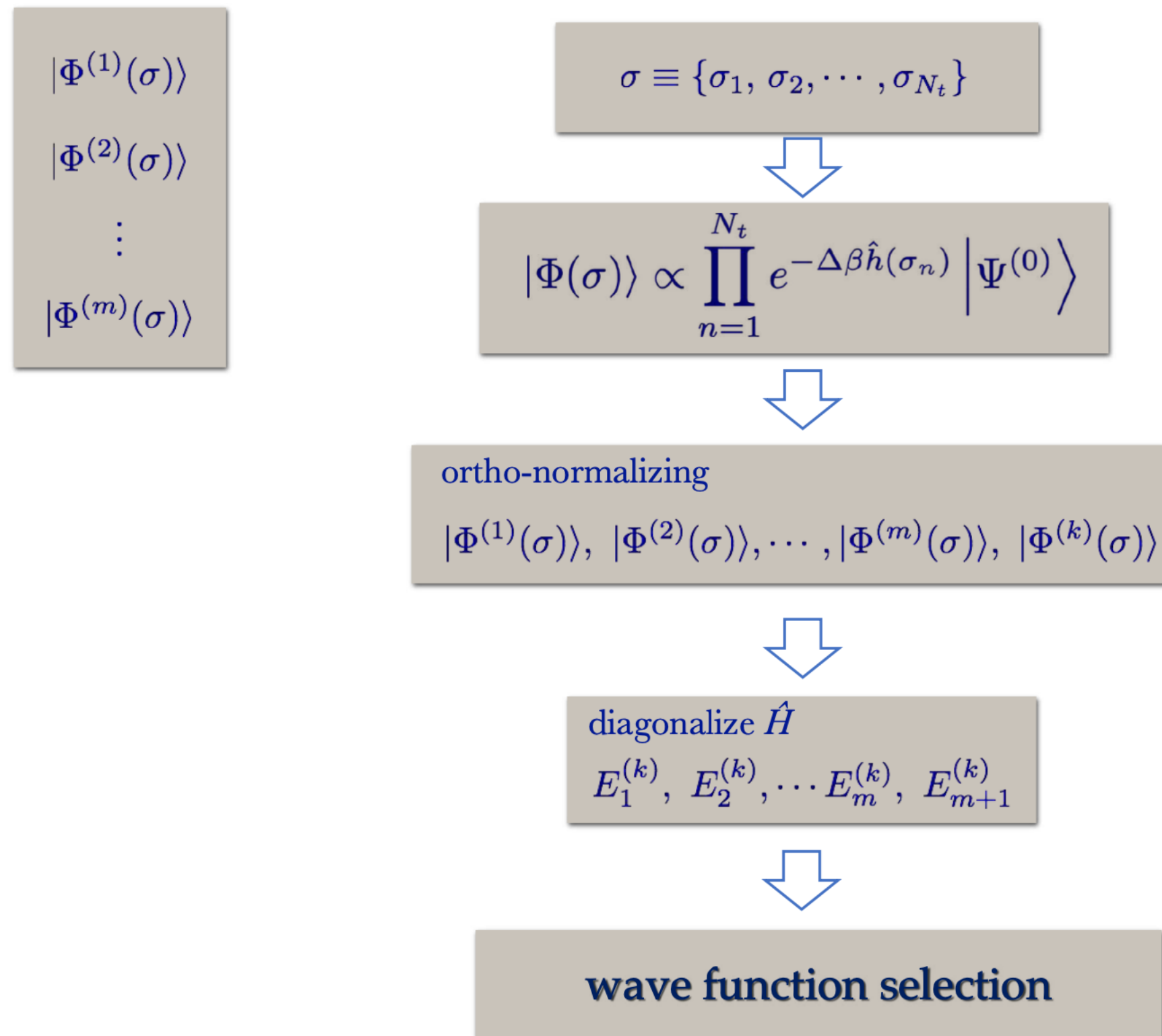


MCSM — Generation Process for Basis





MCSM — Generation Process for Basis



MCSM Bases

MCSM bases

MCSM dimension: the number of bases.

$$|\Phi^{(1)}(\sigma)\rangle$$

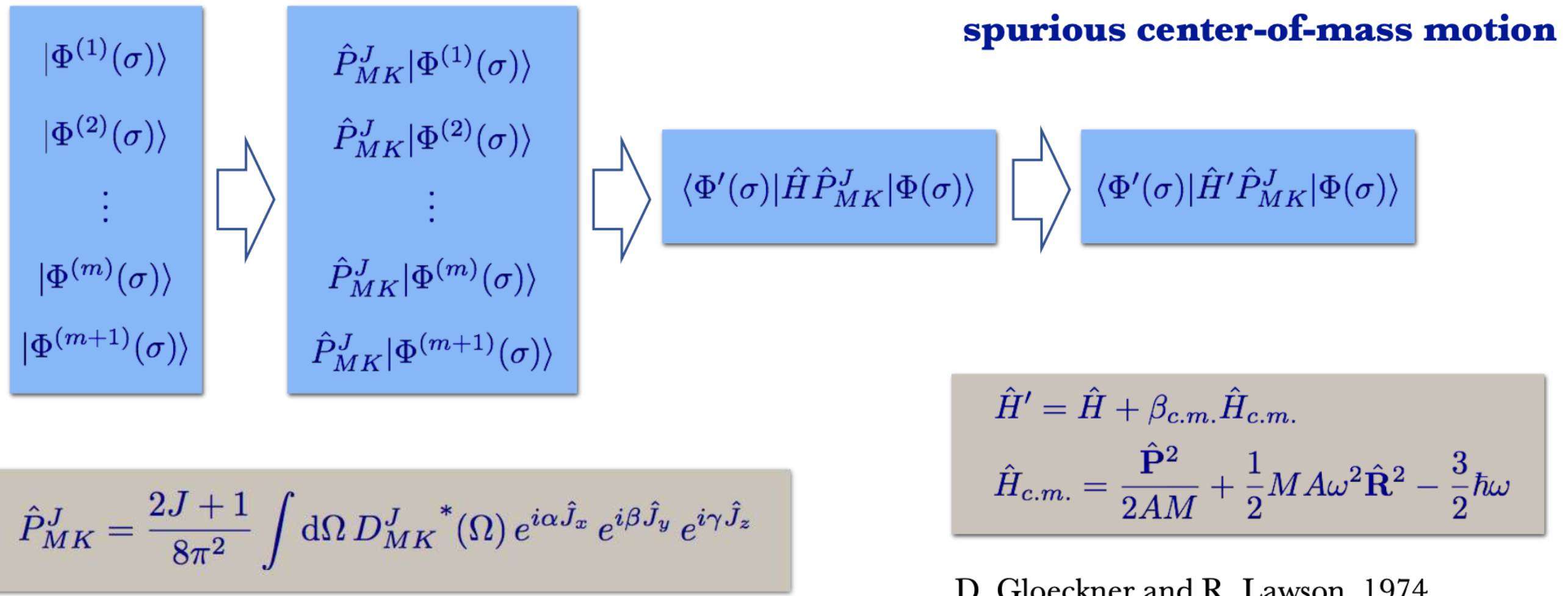
$$|\Phi^{(2)}(\sigma)\rangle$$

⋮

$$|\Phi^{(m)}(\sigma)\rangle$$

$$|\Phi^{(m+1)}(\sigma)\rangle$$

MCSM — Restoration of Symmetry



Monte Carlo shell model

Dimension of H matrix for MCSM

Standard shell model

$$H = \begin{pmatrix} * & * & * & * & * & \dots \\ * & * & * & * & & \\ * & * & * & & & \\ * & * & * & & & \\ * & * & & \ddots & & \\ * & & & & & \\ \vdots & & & & & \end{pmatrix} \xrightarrow{\text{Diagonalization}} \begin{pmatrix} E_0 & & & & & 0 \\ & E_1 & & & & \\ & & E_2 & & & \\ & & & \ddots & & \\ 0 & & & & & \end{pmatrix}$$

Large sparse matrix $\sim \mathcal{O}(10^{10})$

non-zero MEs $\sim \mathcal{O}(10^{13-14})$

Monte Carlo shell model

Importance truncation

$$H \sim \begin{pmatrix} * & * & \cdots \\ * & \ddots & \\ \vdots & & \end{pmatrix} \xrightarrow{\text{Diagonalization}} \begin{pmatrix} E'_0 & & 0 \\ & E'_1 & \\ 0 & & \ddots \end{pmatrix}$$

Important bases stochastically selected

$\sim \mathcal{O}(100)$

T. Otsuka et al., Prog. Part. Nucl. Phys. 47, 319 (2001)

The Extended Kuo-Krenciglowa (EKK) method

- a version of many-body perturbation theory
- starting from a bare nuclear force to derive an effective interaction designed for a given model space (for example, the sd or sd-pf shells)

Problem of the KK method: divergence of the perturbative expansion for a model space composed of more than one major shell.

The EKK method has overcome this difficulty by resumming the perturbative series so that one can avoid the divergence.

- The resummation is performed with a formula similar to the Taylor expansion but in the operator form.
- One can avoid the divergence by choosing an appropriate value of the ‘origin’ of the expansion, without changing the result, as long as the summation of the series converges.



Numerical details

EEdf1 interaction and its single-particle energies

The first application of the EKK method was carried out for the study of the nuclei around the island of inversion, as described in ref.⁴. We outline here how the effective interaction for the shell model calculation was constructed.

The χ EFT interaction proposed by Entem and Machleidt^{22,53} was taken with $\Lambda = 500$ MeV, as the nuclear force in vacuum mentioned above, up to the next-to-next-to-next-to-leading-order (N3LO) in the χ EFT. It was then renormalized by the $V_{\text{low}k}$ approach^{54,55} with a cutoff of $\Lambda_{\text{low}k} = 2.0 \text{ fm}^{-1}$, in order to obtain a low-momentum interaction decoupled from high-momentum phenomena. This treatment helps to generally improve the convergence of the many-body perturbation theory calculation, which is in this case, the EKK method. The EKK method was then adopted in order to obtain the effective NN interaction for the *sd-pf* shell, by including the so-called \hat{Q} -box, which incorporates unfolded effects coming from the outside of the model space⁵¹, up to the third order and its folded diagrams. As the single-particle basis vectors, the eigenfunctions of the three-dimensional harmonic oscillator potential were taken as usual. On top of this, the contributions from the Fujita–Miyazawa 3NF were added in the form of the effective NN interaction. The Fujita–Miyazawa force²⁴ represents effects of the virtual excitation from a nucleon to a Δ baryon by pion-exchange processes. It has been discussed and included in many works, for instance^{56,57}. While the 3NFs may contain other terms, the Fujita–Miyazawa force is considered to produce dominant contributions to binding energies, as shown, for instance, in ref.²³. Furthermore, its major and important roles have recently been clarified also from the viewpoint of the χ EFT interaction⁵⁸. The other terms are still under discussions with variations of their strength parameters among different χ EFT approaches, and their effects are expected to be small with respect to the present issues. We thus retained the Fujita–Miyazawa force in evaluating contributions from the 3NFs, but other 3NFs will be discussed later.

This interaction has been derived via the extended Kuo–Krenciglowa (EKK) method, from the fundamental chiral–effective–field–theory (χ EFT) interaction by Machleidt and Entem stemming from quantum chromodynamics (Methods).

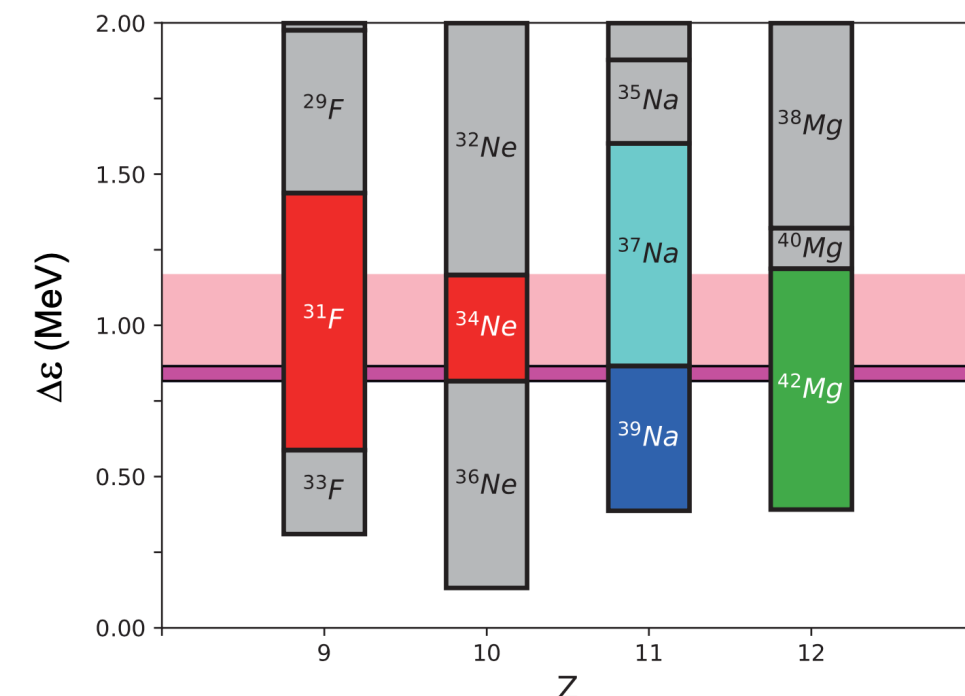
The contributions from three-nucleon forces (3NF) are further included into this effective NN interaction, where the 3NF represents effects of virtual excitations to the Δ particle, that is, the Fujita–Miyazawa force (Methods). The present effective interaction, called EEdf1, is thus constructed

The effective NN interaction for the sd - pf shell was thus constructed, and was named the EEdf1 interaction. There are seven single-particle orbits in the sd - pf shell. Their single-particle energies are determined by the fit, as stated in the main text. We note that only the single-particle energies are fitted and the interaction between valence nucleons in the sd - pf shell is derived as mentioned above. Because of the isospin symmetry, a proton orbit has the same energy as the corresponding neutron orbit except for the Coulomb contribution, which is assumed to be equal to all proton orbits (for a given nucleus) as usual. The values of the seven single-particle energies were determined so as to reproduce observables such as the ground-state energies of $N < 20$, the 2_1^+ level of ^{30}Ne , ^{32}Mg , ^{34}Si , and the excitation energies of several states of ^{31}Mg . The fit was not like a χ^2 -fit but was done so as to reproduce basic patterns of these observables. The single-particle energies of the $2p_{1/2}$ and $1f_{5/2}$ orbits are constrained by the GXPF1 values⁵⁹, as described also in ref.⁴. We note that no structure data of neutron-rich exotic nuclei with $N > 20$ were used in this fit.

Numerical details

The EEdf1 interaction and the single-particle energies attached to it were thus constructed. It has been extensively applied to a variety of cases: many experimental data other than those used for the fit are described well, as one can find not only in Figs. 3, 4, but also in the results shown in refs. ^{4,27–32}.

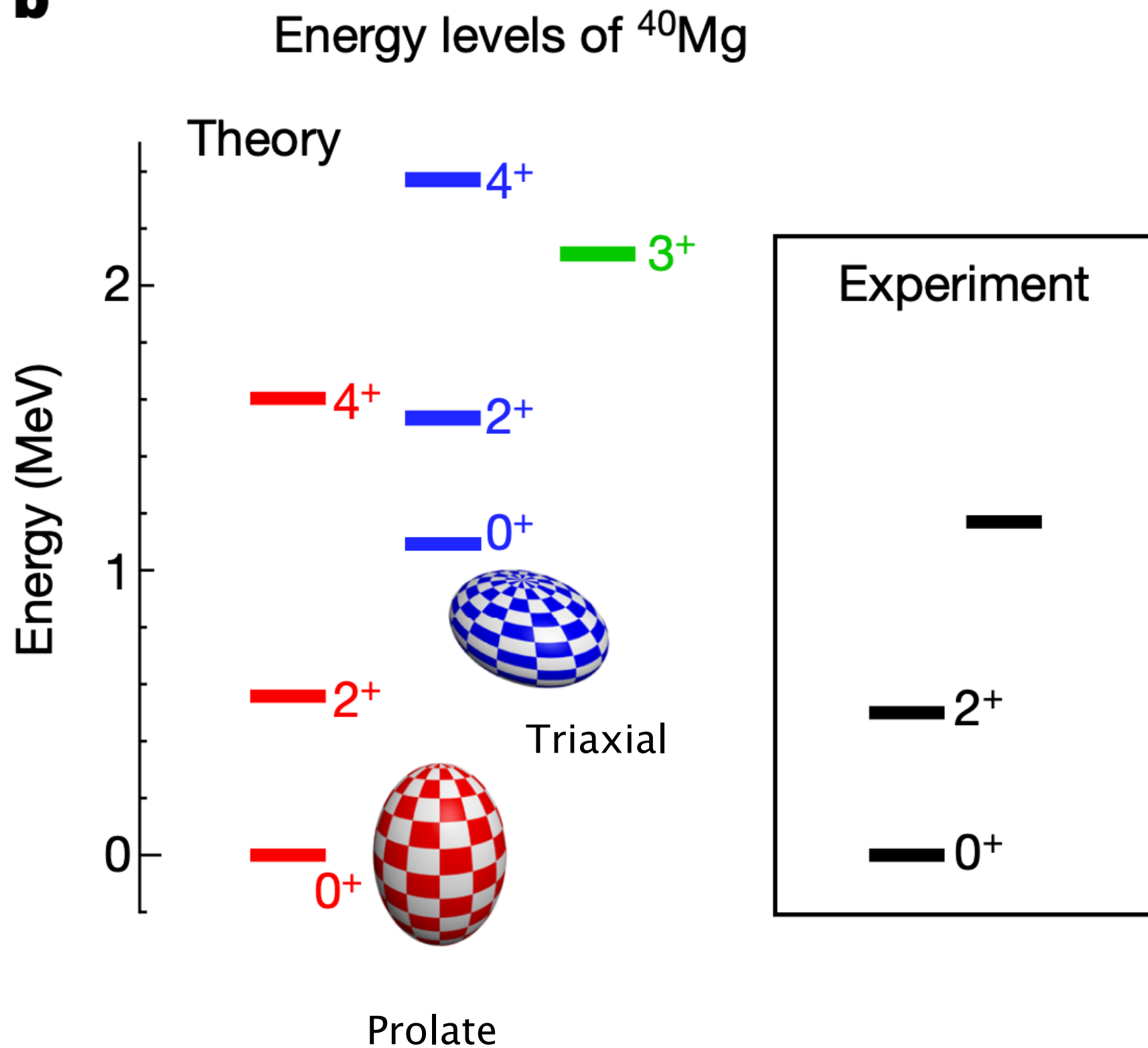
As stated in the main text, the single-particle energies need to be refined from the original EEdf1 values. In the present work, we shift them by the same amount, $\Delta\epsilon$. We first investigate, for each isotopic chain, which nucleus becomes the dripline as a function of $\Delta\epsilon$. As shown in Extended Data Fig. 1, the original values of the single-particle energies ($\Delta\epsilon = 0$) are too low, and the calculated dripline appears too far from the experimentally observed location in the Segrè chart. By increasing the $\Delta\epsilon$ value, the dripline is shifted to smaller N values, that is, to lighter isotopes (Extended Data Fig. 1). The driplines were assigned experimentally to ^{31}F and ^{34}Ne very recently³⁹, suggesting the range $\Delta\epsilon = 0.82\text{--}1.17 \text{ MeV}$. Regarding the chain of Na isotopes, a preliminary report indicates, with one event, that ^{39}Na is bound³⁹. The nucleus ^{37}Na is known to be bound⁶⁰. If the dripline is on ^{39}Na , $\Delta\epsilon = 0.82\text{--}0.87 \text{ MeV}$ is obtained (dark pink belt in Extended Data Fig. 1). As it is very unlikely from empirical systematics that ^{41}Na is bound, we exclude this possibility. We thus adopt $\Delta\epsilon = 0.82 \text{ MeV}$, the lower boundary of the range. This range, 0.050 MeV, is the uncertainty of this study and limits, for instance, the precision of the one-neutron separation energy; it is too small to be visible in Extended Data Fig. 1. The ^{40}Mg isotope is known to be bound⁶¹, and the predicted dripline of Mg isotopes is ^{42}Mg (Extended Data Fig. 1).



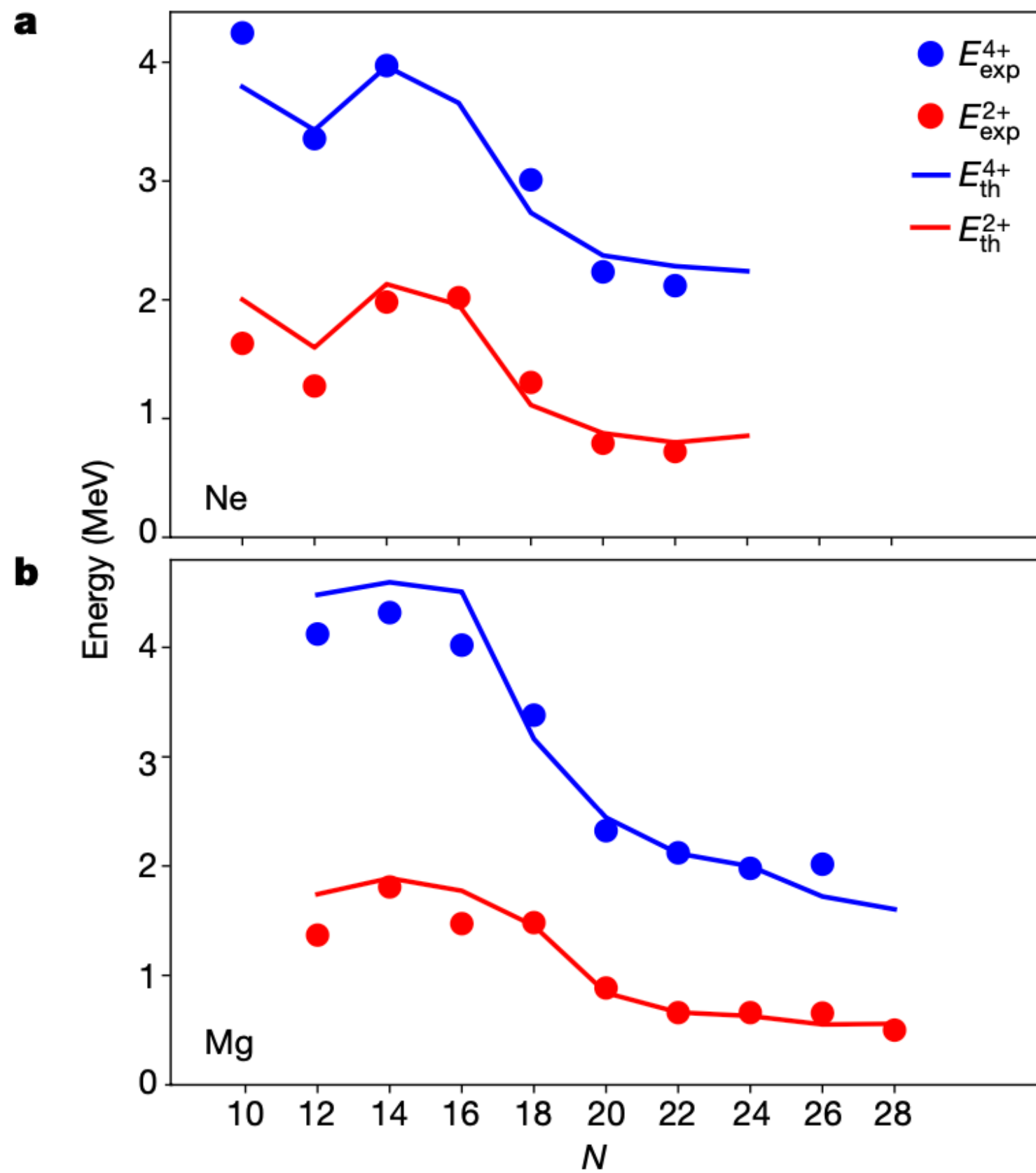
Results and discussion



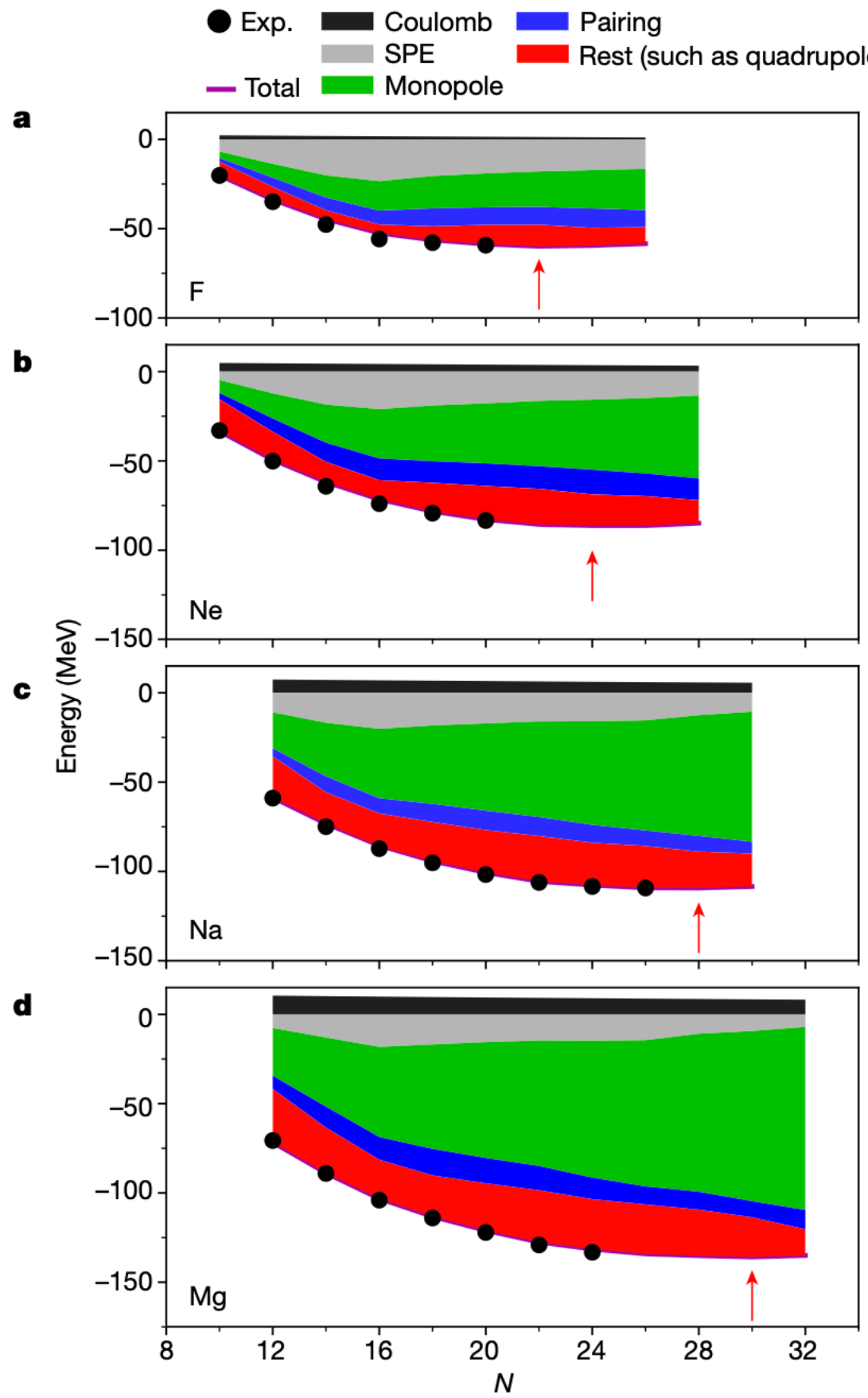
b



Results and discussion



Results and discussion



Decomposition of the interaction

A given effective NN interaction, v_{NN} , scatters a pair of nucleons in single-particle orbits j_1 and j_2 into a pair of single-particle orbits j_3 and j_4 , conserving their total angular momentum and parity π . The isospin T is relevant also, but is omitted here. This process is expressed by the so-called two-body matrix element

$$\langle j_3, j_4 ; J^\pi | v_{NN} | j_1, j_2 ; J^\pi \rangle. \quad (2)$$

$$v_{NN} = v_{\text{mono}} + v_{\text{pair}} + v_{\text{rest}}$$

Monopole term:

$$V^m(j_1, j_2) = \frac{\sum_J (2J+1) \langle j_1, j_2 ; J^\pi | v_{NN} | j_1, j_2 ; J^\pi \rangle}{\sum_J (2J+1)},$$

Pairing term:

$$\langle j_3, j_3 ; J^\pi = 0^+ | v_{NN} - v_{\text{mono}} | j_1, j_1 ; J^\pi = 0^+ \rangle.$$

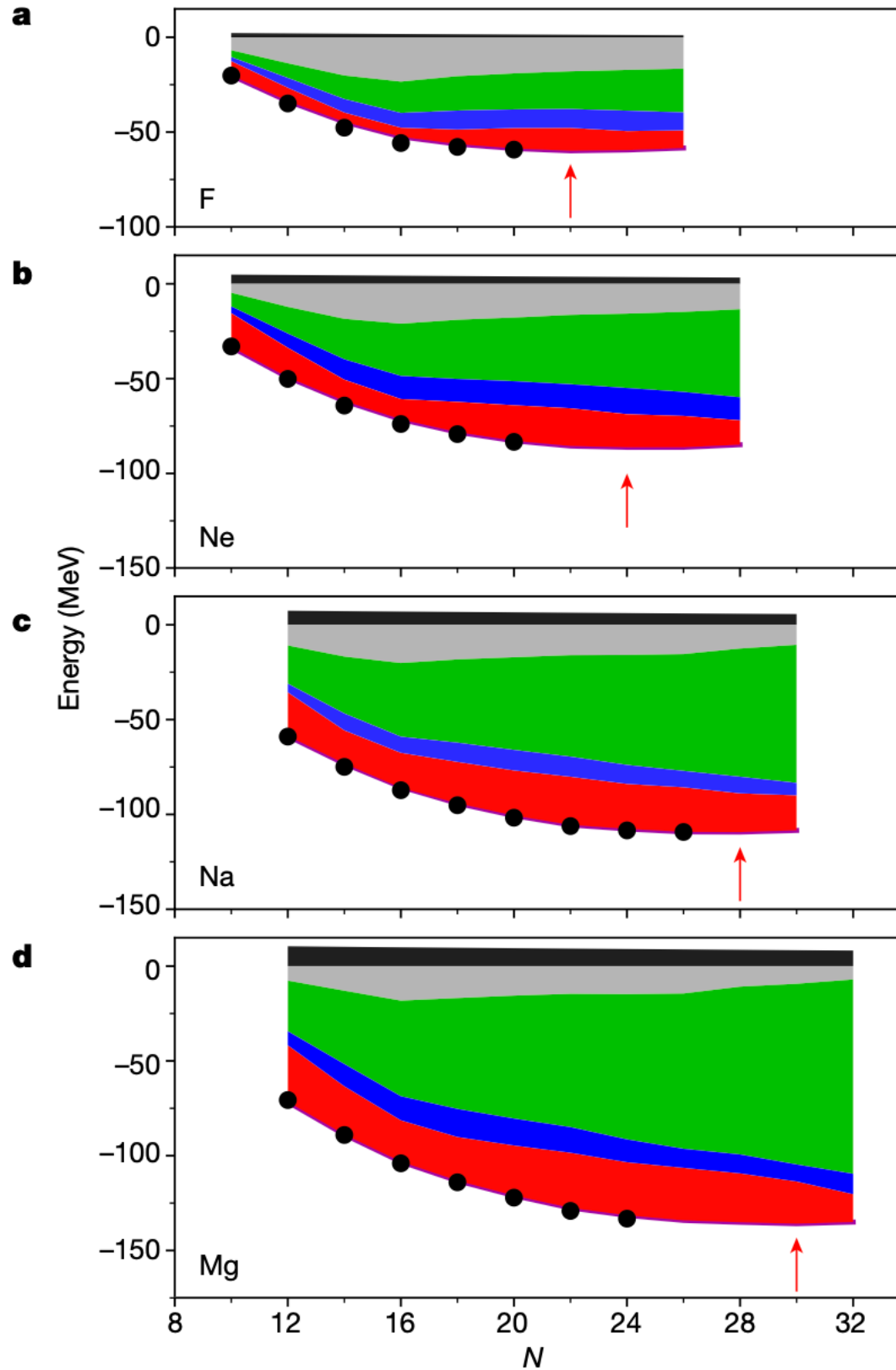
The rest interaction is given by:

$$v_{\text{rest}} = v_{NN} - v_{\text{mono}} - v_{\text{pair}}$$

Results and discussion

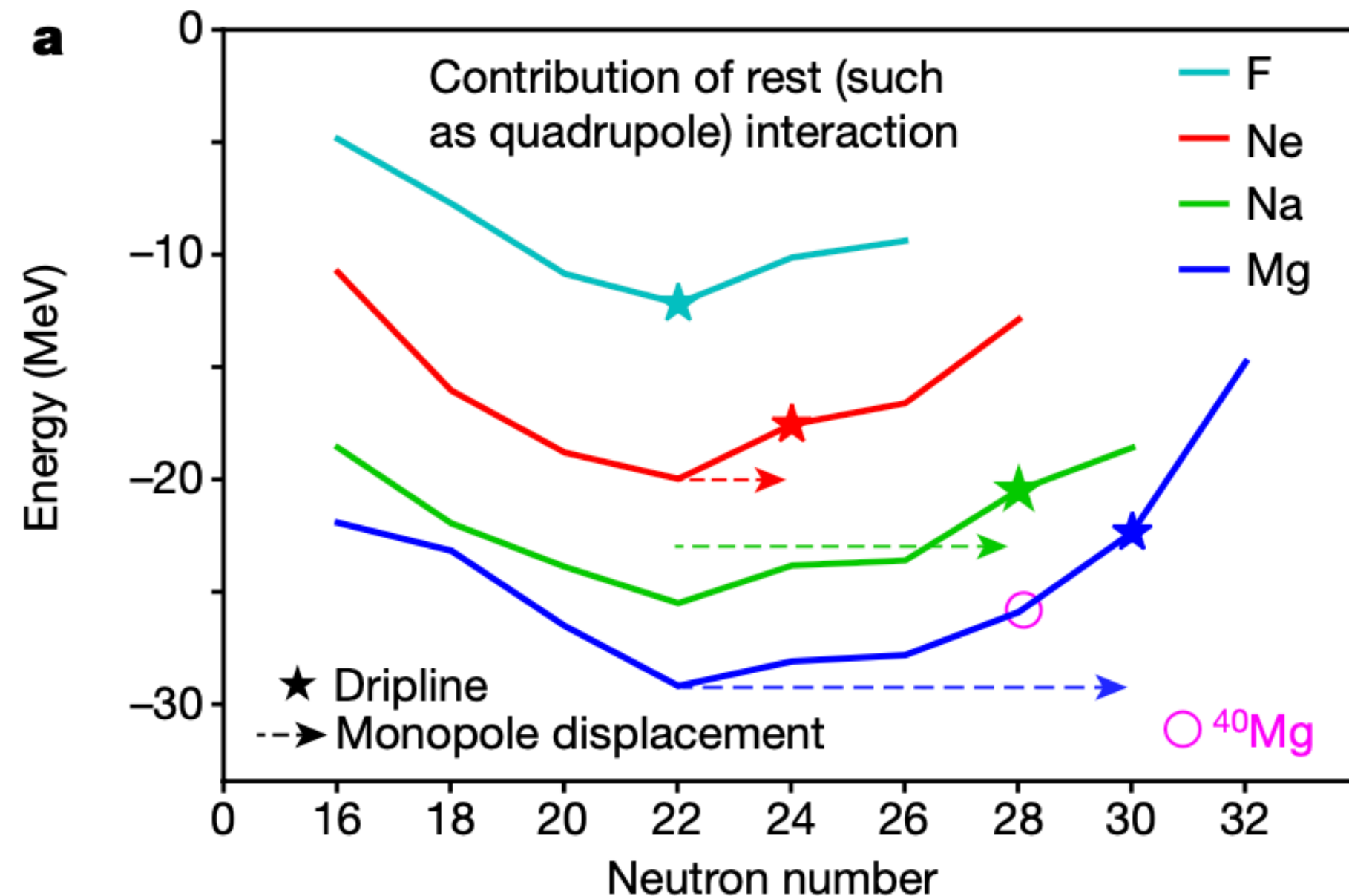


● Exp. Coulomb Pairing
 SPE Rest (such as quadrupole)
— Total Monopole



We calculate the ground-state energies relative to that of the ^{16}O nucleus and compare them to experimental data (Fig. 4). A good agreement is seen in each panel. Although the NN interaction was derived as described above, the single-particle energies with respect to the ^{16}O inert core were fitted as free parameters for the original EEdf1 Hamiltonian⁴ (Methods). In principle, the single-particle energies can be derived, but more studies are needed to achieve an accuracy comparable to that of the effective NN interaction. The validity of these fitted values has been confirmed by comparison to a number of experimental data not only of energy levels but also of electromagnetic properties or spectroscopic factors^{4,28–32}. Although the derivation of the effective NN interaction does exhibit a certain ab initio aspect, this fit prevents us from calling the present calculation fully ab initio.

Results and discussion



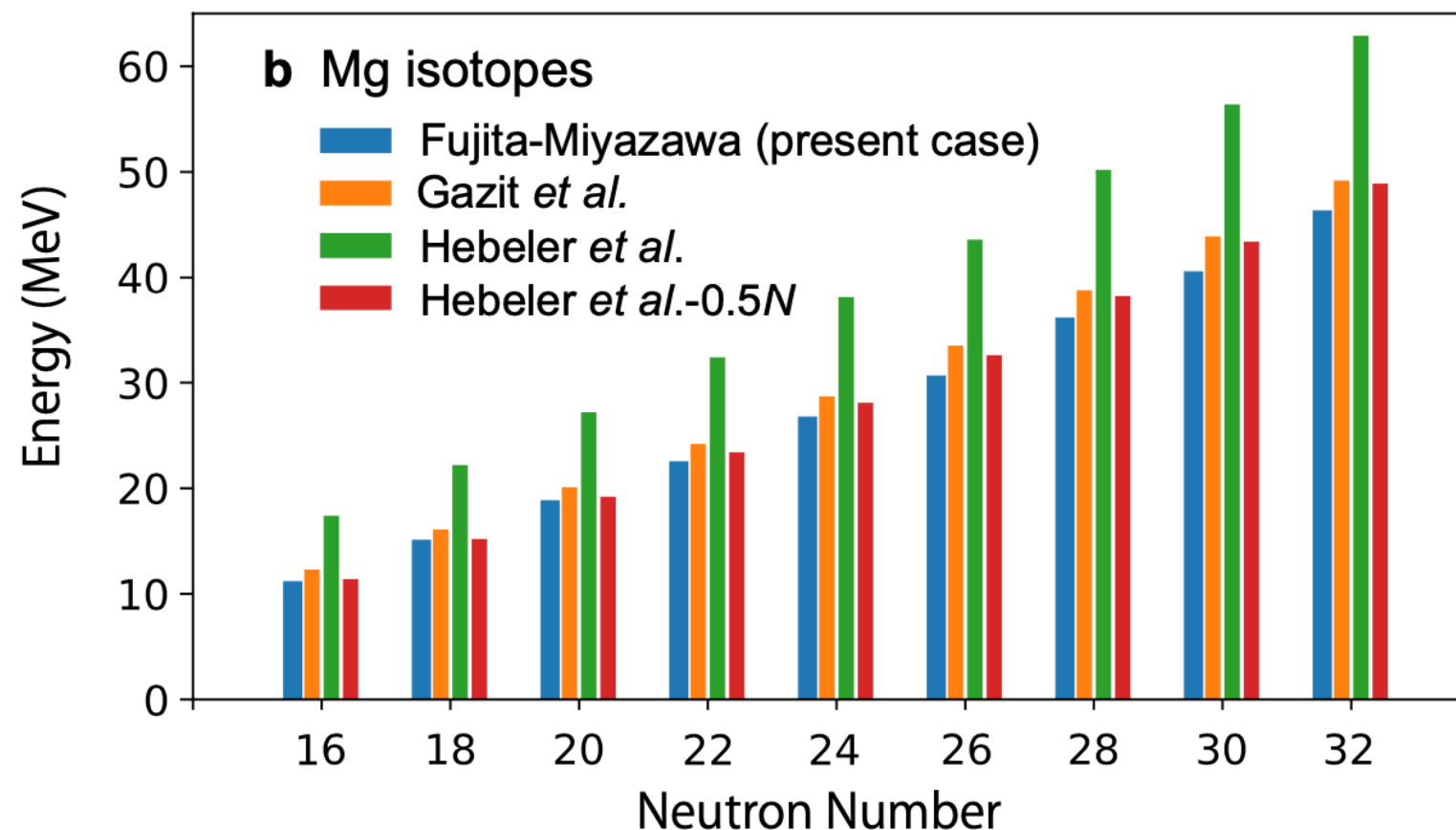
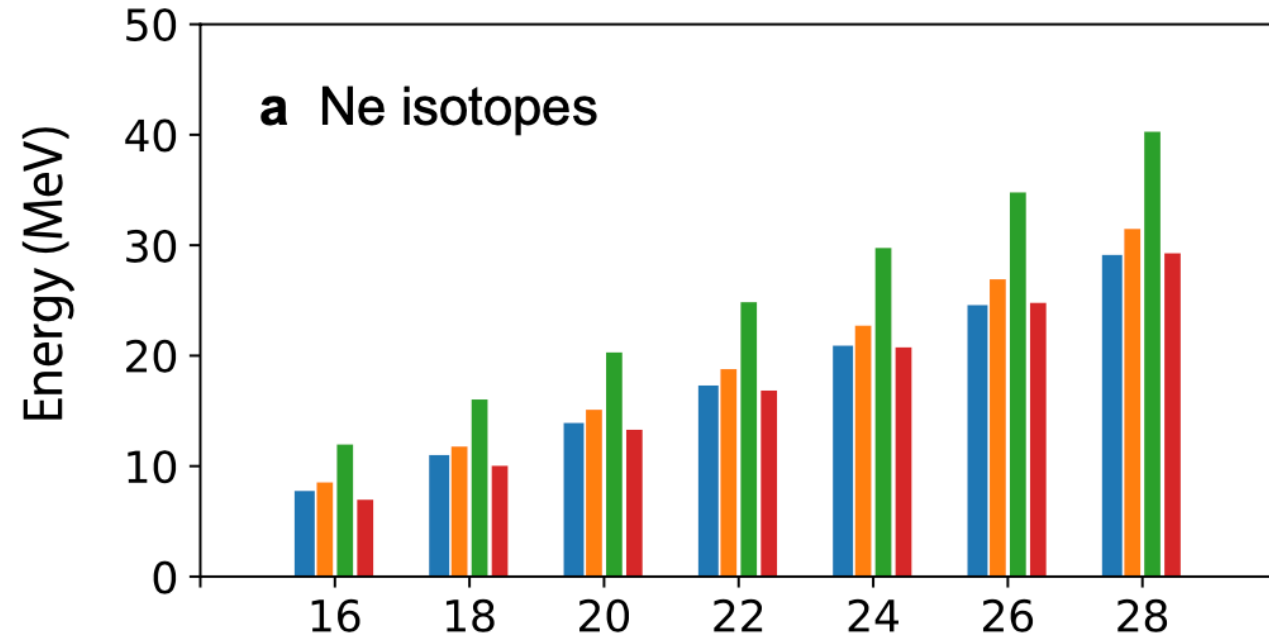
Contributions of

- the rest (四极形变能为主) component of the NN interaction (solid)
- Single-particle energy plus monopole effects (dashed)

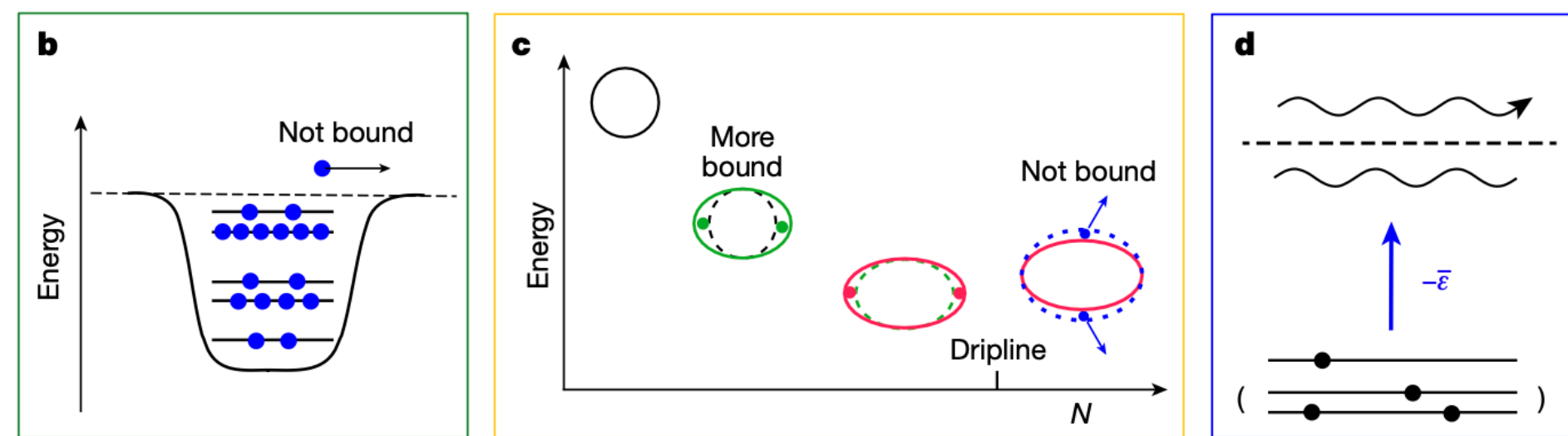
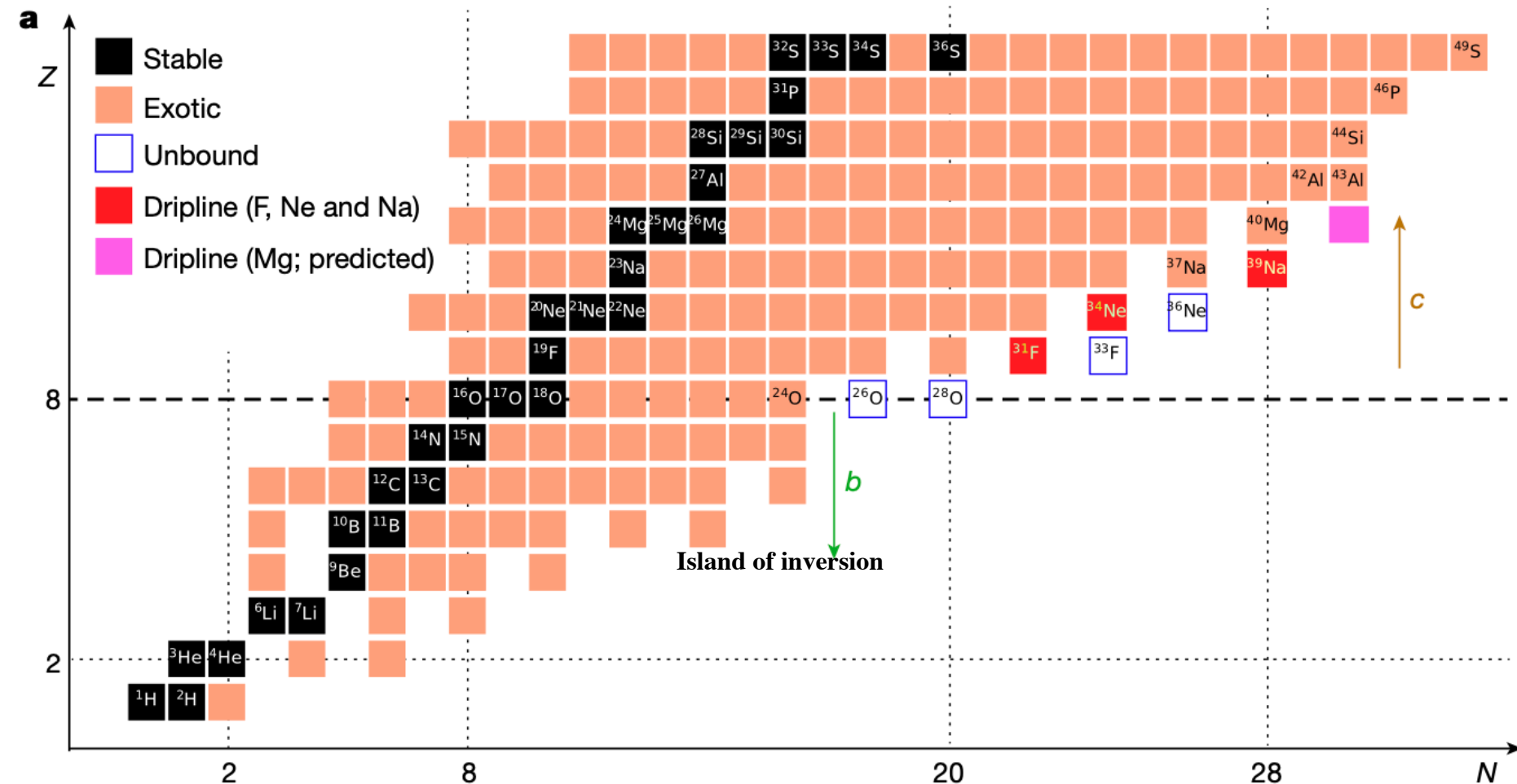
Results and discussion



Ground-state expectation value of the 3NF for the Ne and Mg isotopes.



Results and discussion



Traditional dripline mechanism

New dripline mechanism

Neutron separation energy



Summary

Prospects

Here we have described a mechanism for the dripline of atomic nuclei, to which both the variation of the shape deformation and the combined-monopole effect contribute. Although this mechanism is not very sensitive to details, the agreement with a variety of experimental data and the *ab initio* nature of the effective NN interaction enhance the reality of the mechanism. The patterns of the monopole and rest effects in Fig. 4 have been observed in other regions of the Segrè chart²⁷, and their combination, naturally and robustly, gives us the present dripline mechanism, in which the EEdf1 interaction provides their precise magnitudes. It is remarkable that the driplines of F, Ne and probably Na isotopes are described within a single framework of EEdf1 interaction, despite the large structural changes observed. The excited states are described also, including the recent data for ^{40}Mg . As a general outcome, this work proposes two dripline mechanisms: one with a single-particle nature and the other with shape deformation (the collective mode), as shown in Fig. 2b, c, respectively. These two mechanisms are complementary, and may appear alternatively as Z increases. For instance, the mechanism in Fig. 2b may return for the magic number $Z \approx 20$. The interplay of single-particle versus collective aspects has been studied in many facets of nuclear structure^{49,50}, and is now shown to be crucial also to the dripline. Including intermediate situations, it is of great interest where and how these two mechanisms arise as Z changes as well as how one can observe them experimentally, for example, by measuring ellipsoidal deformation of the nuclei towards driplines. The relation between fission and the present mechanism is of interest as the limiting case of the dripline in heavy nuclei.